Chemical Science

ROYAL SOCIETY OF CHEMISTRY

EDGE ARTICLE

View Article Online
View Journal | View Issue

Cite this: *Chem. Sci.*, 2024, **15**, 18557

All publication charges for this article have been paid for by the Royal Society of Chemistry

Photoinduced copper-catalyzed asymmetric cyanoalkylalkynylation of alkenes, terminal alkynes, and oximes†

Shuang Xin, Jibang Liao, Qi Tang, Xiaoming Feng and Xiaohua Liu *

The asymmetric dicarbofunctionalization of alkenes *via* a radical relay process can provide routes to diverse hydrocarbon derivatives. Three-component carboalkynylation, limited to particular alkyl halides and using readily available cycloketone oxime esters as redox-active precursors, is restricted by the available pool of suitable chiral ligands for broadening the redox potential window of copper complexes and simultaneously creating the enantiocontrol environment. Herein, we report a new hybrid tridentate ligand bearing a guanidine–amide–pyridine unit for photoinduced copper-catalyzed cyanoalkylalkynylation of alkenes. Leveraging the copper catalyst's redox capability is achieved *via* merging the electron-rich ligand with a readily organized configuration and enhanced absorption in the visible light range, which also facilitates the enantioselectivity. The generality of the catalyst system is exemplified by the efficacy across a number of alkenes, terminal alkynes and cycloketone oxime esters, working smoothly to give alkyne-bearing nitriles with good yields and excellent enantioselectivity. A mechanistic study reveals that the chiral copper catalyst meets the requirements of possessing sufficient reduction ability, good light absorption properties, and appropriate steric hindrance.

Received 22nd August 2024
Accepted 13th October 2024

DOI: 10.1039/d4sc05642f

rsc.li/chemical-science

Introduction

Alkene difunctionalization is widely recognized as a pivotal approach in organic synthesis owing to its unique ability to introduce molecular complexity in a single synthetic step.[1] Transition-metal-catalyzed three-component alkene dicarbofunctionalization *via* a radical relay approach has gained significant traction,[2] but asymmetric catalytic versions enabling construction of chiral carbon centers are still scarce. Chiral copper-catalyzed alkylcyanation, alkylarylation and alkylalkynylation (Scheme 1a) of styrenes using alkyl halides,[3] Togni reagents,[4] alkyl peroxides,[5] or alkyl *N*-hydroxyphthalimide esters[6] as the alkyl radical sources have been realized, usually with the assistance of oxazoline-type ligands, with or without light assistance. The alkylation of terminal alkynes into internal alkynes *via* an enantioselective coupling reaction has drawn great effort,[7] for example using the Sonogashira coupling reaction, as shown in work by the groups of Fu and Eckhardt[8] and by Hwang and Sagadevan,[9] as well as by several other groups, with or without photoinduced copper-catalyzed conditions.[10,11]

Based on these studies, three-component carboalkynylation of olefins *via* an atom transfer radical addition process was also made available (Scheme 1a) by the use of alkyl iodides in

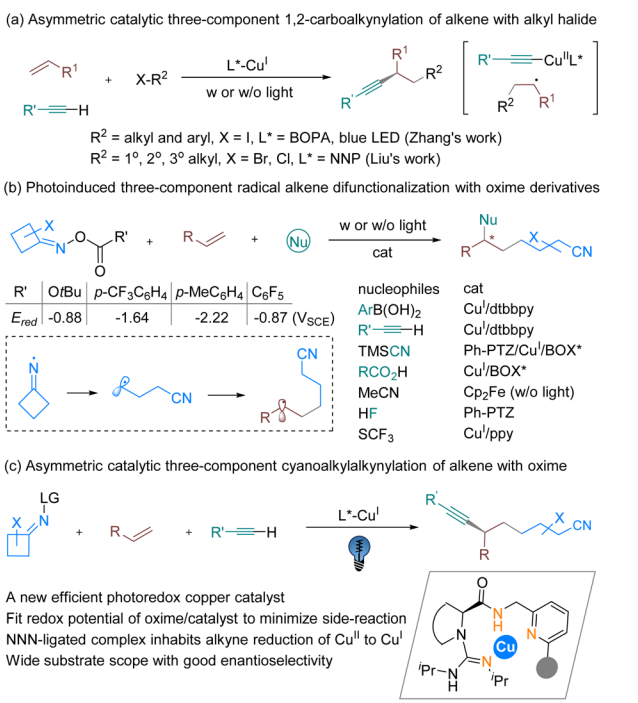

Scheme 1 Difunctionalization of alkenes involving cycloketone oxime esters or terminal alkynes.

Key Laboratory of Green Chemistry & Technology, Ministry of Education, College of Chemistry, Sichuan University, Chengdu 610064, P. R. China. E-mail: liuxh@scu.edu.cn

† Electronic supplementary information (ESI) available: ^{1}H, ^{13}C{^{1}H} and ^{19}F{^{1}H} NMR, HPLC and UPC^{2} spectra. X-ray crystallographic data for **F**. CCDC 2331715. For ESI and crystallographic data in CIF or other electronic format see DOI: https://doi.org/10.1039/d4sc05642f

Zhang's study[3b] and electron-withdrawing substituted alkylhalides in Liu's work.[3a]

Cycloketone oxime esters as sources of cyanoalkyl radicals have been extensively explored for synthesizing a broad range of functionalized alkylnitriles,[12] pioneered by Zard's research.[13] A variety of difunctionalizations of alkenes using oxime esters as viable coupling partners have been disclosed by Xiao's group and others (Scheme 1b).[14] In comparison with alkyl halides as the radical precursors, the generation of cyanoalkyl radicals provides an improvement *via* a higher reductive potential and an additional cleavage process from iminyl radicals delaying the radical relay process. Special features of copper complexes under UV irradiation[2a,15] provide the ability to accelerate difunctionalization with oxime esters, where in most cases copper photocatalysts bearing particular ligands or combined with an exogenic photocatalyst are able to initiate a single-electron transfer (SET) process to generate a radical species (Scheme 1b). Asymmetric catalytic transformations have been limited to TMSCN[14f] and carboxylic acid[14c] as the nucleophilic partners, and aryl boronic acid as the coupling partner has just been reported very recently;[16] therefore the process of asymmetric cyanoalkylalkynylation of olefins remains an open subject (Scheme 1c). Although copper acetylides could advance SET by means of a UV-light-absorbing photocatalyst,[9,17] the terminal alkyne could reduce the formed Cu(II) species to Cu(I), intruding upon the desired alkylalkynation reaction.[18] In addition, side reactions, such as direct coupling between the cyanoalkyl radical and nucleophilic reagents, and dimerization, would accompany the process.[19] Therefore, introducing suitable chiral ligands to modulate the reactivity of the excited copper acetylide complex, and to discriminate the sterically hindered aryl/cyanoalkyl subunit of the radical intermediate for enantioselective coupling, is critical.

The variety of chiral ligands that can straightforwardly support copper-catalyzed photoreactions in a stereocontrolled manner is consequently somewhat limited to a handful N- or P-based heteroleptic compounds.[20] It is important that the chiral ligand must stabilize the copper complex in specific oxidation states and electronic configurations. Inspired by the entatic-state principle, which has been applied to copper electron-transfer processes[21] *via* lowering the reorganization energy during redox processes, thus facilitating a fast electron transfer, we rationalized that tridentate hybrid N-donor ligands containing a guanidine,[22,23] amide and pyridine subunit (Scheme 1c), which has been disclosed to accelerate Sonogashira coupling of alkyl bromides,[24] are also potential ligands for copper-based photocatalysts. Multiple donors and ready modification of the substituents of the ligand are useful to increase the rigidity for pre-organizing the configuration, and a methylene linker between the amide and pyridine provides some conformational flexibility. Further, taking multiple N-donor characters together, these kinds of ligands have a preference for stabilizing copper in various oxidation states. Additionally, these subunits are thought of as redox non-innocent, which may contribute to changes in the electronic nature of the metal center and contribute to reactivity. Herein, we describe the development of a new chiral photoredox copper catalyst for a general three-component radical 1,2-cyanoalkylalkynylation of alkenes with cycloketone oxime esters and terminal alkynes.

Results and discussion

Our initial survey started with alkylalkynylation of 2-vinylnaphthalene **B1** with Cu(I)/chiral guanidine as the catalyst in the presence of Cs_2CO_3 and under irradiation by 3 W blue LEDs, and cyclobutanone *O*-(4-methoxybenzoyl) oxime **A1** and phenylacetylene **C1** were used as the cyanoalkyl reagent and alkynyl reagent, respectively. As shown in Table 1, the desired three-component coupling product **D1** could be obtained with moderate enantioselectivity and a low yield in tetrahydrofuran (THF) at 20 °C upon irradiation with 440 nm light (entries 1–5). Competitive formation of two-component coupling byproducts between a nitrogen-centered radical or cyanoalkyl radical and the terminal alkyne (**BP-1** and **BP-2**) accounted for the unsatisfactory yield. It was delightful that the addition of a phenyl substituent at the *ortho*-position of the methylpyridine subunit of the ligand (**G-TqPy-3**) led to increased enantioselectivity with a slightly higher yield (entry 3). When the reaction was conducted with CuOTf as the metal precursor, the

Table 1 Optimization of the reaction conditions[a]

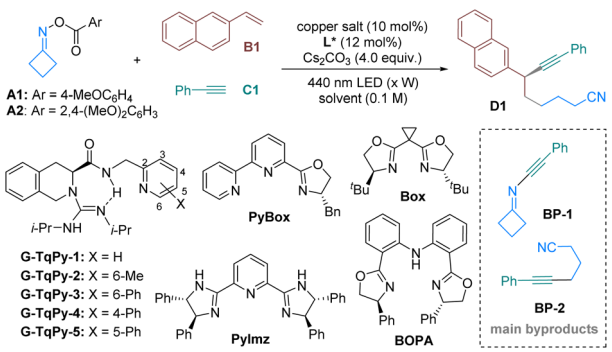

Entry[a]	Conditions	Yield[b] (%)	ee[c] (%)
1	**A1**, **G-TqPy-1**, CuI, THF, (3 W)	22	45
2	**A1**, **G-TqPy-2**, CuI, THF, (3 W)	24	49
3	**A1**, **G-TqPy-3**, CuI, THF, (3 W)	38	74
4	**A1**, **G-TqPy-4**, CuI, THF, (3 W)	18	45
5	**A1**, **G-TqPy-5**, CuI, THF, (3 W)	20	45
6	**A1**, **G-TqPy-3**, CuOTf, THF, (3 W)	38	81
7[d,e]	**A1**, **G-TqPy-3**, CuOTf, (3 W)	34	91
8[d,f]	**A1**, **G-TqPy-3**, CuOTf, (10 W)	51	87
9[d,f]	**A2**, **G-TqPy-3**, CuOTf, (10 W)	52	91
10[d,f]	**A2**, **BOPA**, CuOTf, (10 W)	23	35
11[d,f]	**A2**, **Box**, CuOTf, (10 W)	Trace	—
12[d,f]	**A2**, **PyImz**, CuOTf, (10 W)	Trace	—
13[d,f]	**A2**, **PyBox**, CuOTf, (10 W)	Trace	—

[a] Unless otherwise noted, all reactions were performed with [Cu]/**L*** (1 : 1.2, 10 mol%), **A** (3.0 equiv.), **B1** (0.1 mmol), **C1** (3.0 equiv.) and Cs_2CO_3 (4.0 equiv.) in THF (1.0 mL) at 20 °C for 24 h, with 440 nm LED irradiation. [b] NMR yield using 1,1,2,2-tetrabromoethane as an internal standard. [c] The ee values were determined *via* ultraperformance convergence chromatography (UPC²). [d] In PX/DCM (v/v = 7/3, 1.0 mL) for 44 h. [e] At 0 °C. [f] At 5 °C.

enantioselectivity could be improved to 81% ee (entry 6). In a mixed solvent of *p*-xylene (PX) and dichloromethane (DCM) at 0 °C, a 91% ee was obtained but the yield remained unsatisfactory (entry 7). Initiation with stronger light (10 W) could increase the yield at 5 °C, but the enantioselectivity slightly dropped (entry 8). If **A2** was used as the cyanoalkyl reagent, it participated in the reaction to give a 52% yield and 91% ee (entry 9). Further ligand screening *via* the exchange of several classic nitrogen-based oxazoline or imidazoline ligands revealed that the reaction was sluggish with neutral nitrogen-based ligands (entries 11–13), while bisoxazoline diphenylaniline (BOPA) served as an exception and could afford the product in 23% yield with 35% ee, accompanied by a lot of two-component byproducts.

With the optimized reaction conditions established, the substrate scope of the terminal alkynes was explored in the presence of CuOTf/**G-TqPy-3** catalyst under 440 nm light irradiation (Scheme 2). Various substituted ethynylbenzenes could undergo the coupling reaction with moderate yields (48–58%) and excellent ee values (85–91%), regardless of the positions and electronic nature (**D2-D12**, and **D17**). Terminal alkynes bearing a substituent such as an alkyl, cyclopropyl or TMS were also tolerable with slightly higher yields (55–60%) and good enantioselectivities (79–85% ee; **D13–D16**). In addition, 2-ethynylnaphthalene and 3-ethynylthiophene could also be installed into the desired products (**D18** and **D19**) with comparable outcomes.

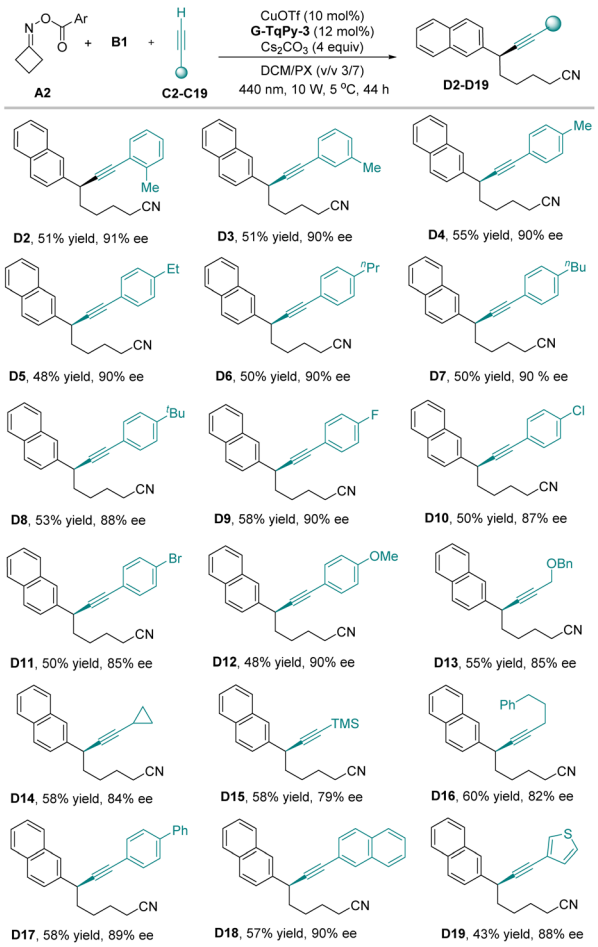

Scheme 2 Substrate scope of terminal alkynes. Unless otherwise noted, all reactions were performed with CuOTf/**G-TqPy-3** (1 : 1.2, 10 mol%), **A2** (3.0 equiv.), **B1** (0.1 mmol), **C** (3.0 equiv.), and Cs_2CO_3 (4.0 equiv.) in PX/DCM (v/v = 7/3, 1.0 mL) under 10 W LED (440 nm) irradiation at 5 °C for 44 h. Isolated yields. The ee values were determined *via* high-performance liquid chromatography (HPLC) on a chiral stationary phase.

Next, we examined the scope of the alkenes and cyanoalkyl reagents (Scheme 3). The investigation of the generality of the alkenes when reacting with **A2** and phenylacetylene **C1** revealed that an array of alkenes was well-tolerated (**D20–D42**). The 6-substituted 2-vinylnaphthalenes bearing electron-donating or -withdrawing groups all worked well (**D20–D22**). The aryl groups could also be hetero-containing ones, such as 5-benzo[*b*]thiophene, 5-benzo[*d*][1,3]dioxole, *N*-tosyl-indole or 5-benzofuran, and the corresponding products (**D23–D26**) could be isolated in 45–55% yield with 82–85% ee. Next, styrene derivatives with electron-donating and -withdrawing substituents at different positions were tested (**D27–D40**), which showed less effect on both the yield (47–64%) and enantioselectivity (83–91% ee), with *para*-O^{t}Bu-substituted **D41** as an exception, which was isolated in reduced yield but with a good ee value. The coupling with 3-vinylthiophene led to the formation of product **D42** in 58% yield and 87% ee. Interestingly, the alkynylated alkene **B25** can provide the corresponding product **D43** in 63% yield with 92% ee. This provides a new method for constructing chiral dialkynyl compounds.

In addition, we continued to examine the cyanoalkyl radical precursors. Mono-substituted cyclobutanone oxime ester **A3**, 4,4-pyridine-substituted **A5** and 3,3-azetidine-substituted **A6** could be delivered into the products (**D44–D46**) bearing substitution at the alkyl-chain, with the results slightly diminished (80–85% ee). Unfortunately, while the bicyclo[4.2.0]octa-1(6),2,4-trien-7-one oxime ester **A4** and 2,2,4,4-tetramethylcyclobutane-1,3-dione oxime ester **A7** could transfer the related cyanoalkyl group into the products, both the yield and ee value dropped significantly (**D47** and **D48**), which might be due to steric hindrance.

In order to evaluate the application potential of this catalytic system, we conducted a scaled-up experiment using **A2**, styrene (**B10**) and phenylacetylene (**C1**) as the substrates (Scheme 4a). Product **D28** could be obtained with a 60% yield (0.92 g) and 90% ee value, indicating the suitability of this catalytic system for gram-scale synthesis. Subsequently, the alkyne group was reduced under Pd/C and H_2 conditions to yield 6,8-diphenyloctanenitrile **E** with 82% yield, maintaining the enantioselectivity. The cyano group was further converted to a carbonyl group, affording 1,6,8-triphenyloctan-1-one **F**, whose absolute configuration was determined to be (*R*)-**F** based on X-ray single-crystal diffraction analysis (Scheme 4a).[25] Thus, the absolute configuration of the product **D28** was rationalized as the (*S*)-isomer.

To detect the radical intermediates generated in the system, EPR experiments and control experiments were conducted (Scheme 4b–d). A solution of oxime **A2** with one equivalent of

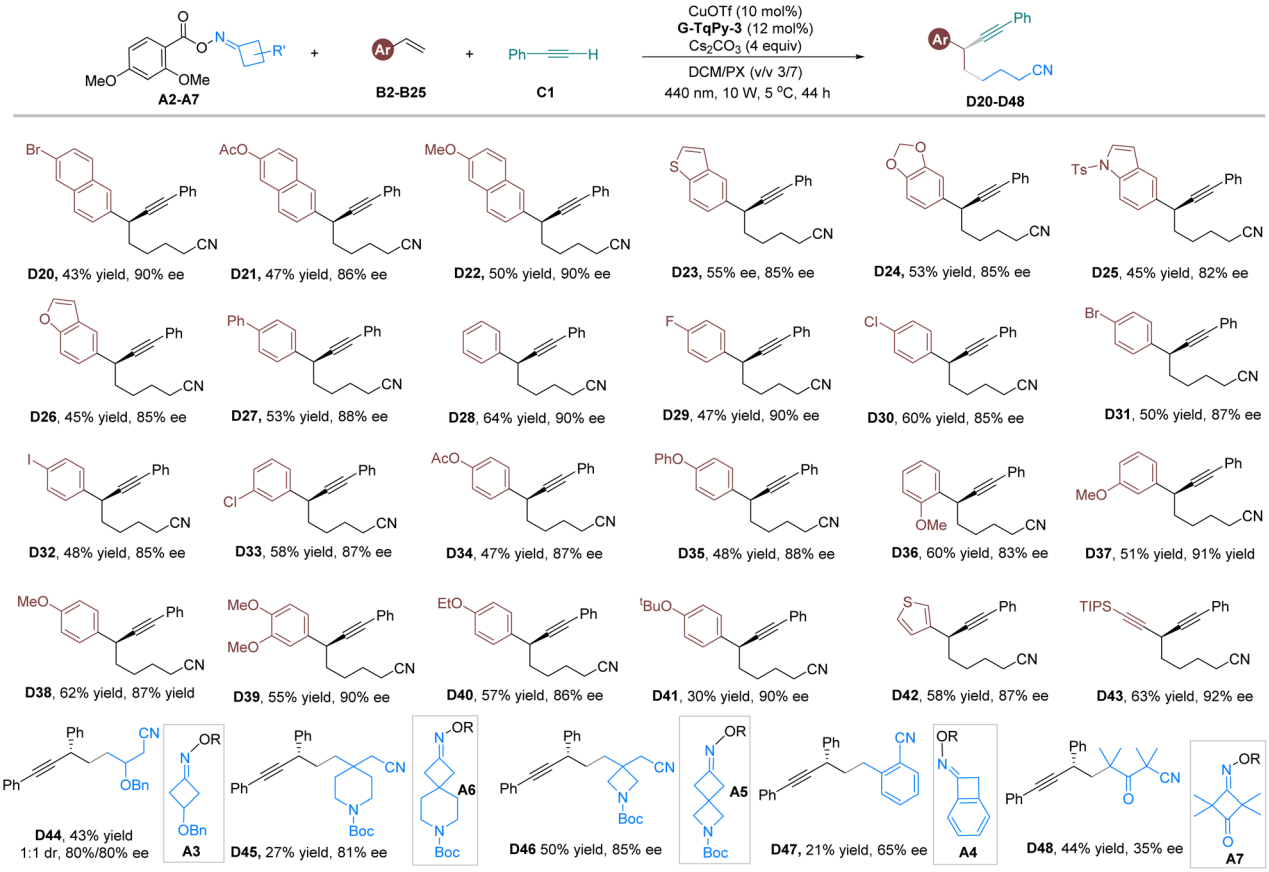

Scheme 3 Substrate scope of alkenes and cycloketone oxime esters. Unless otherwise noted, all reactions were performed with CuOTf/**G-TqPy-oPh** (1 : 1.2, 10 mol%), **A** (3.0 equiv.), **B** (0.1 mmol), **C1** (3.0 equiv.), and Cs_2CO_3 (4.0 equiv.) in PX (0.7 mL) and DCM (0.3 mL) under 10 W LED (440 nm) irradiation for 44 h. Yields are of the isolated products. The ee values were determined *via* HPLC on a chiral stationary phase.

5,5-dimethyl-1-pyrroline-*N*-oxide (DMPO) and chiral copper catalyst in a mixture of *p*-xylene and dichloromethane produced obvious signals under visible-light irradiation. The experimental signals matched the simulated spectra of the mixture of intermediates **H** and **I** (Scheme 4b), indicating the generation of an iminyl radical and the related alkyl radical through a photoinduced copper(I)-catalyzed SET process. When (2,2,6,6-tetramethylpiperidin-1-yl)oxyl (TEMPO) was introduced into the reaction system, the cyanoalkylalkynylation reaction was inhibited and only the radical cross-coupling byproduct **G** was detected *via* ESI-MS and ^{1}H NMR analysis (Scheme 4c). Furthermore, under the standard conditions, when a radical clock experiment was conducted using alkene **B26**, the cyclopropyl group was opened to give product **D49** in a yield of 44% (Scheme 4d), giving evidence of a radical relay process *via* addition to the alkene.

The photophysical and electrochemical properties of the chiral copper complexes prepared *in situ* were investigated. UV-visible absorption spectra of the free ligand and the copper complexes in a dichloromethane solution were recorded (Scheme 4e). This revealed that the absorption above 400 nm increased gradually upon coordination with CuOTf, and the chiral copper acetylide complexes featured a further intense absorption band. The irradiation with 440 nm light enables the formation of excited copper catalytic species. In comparison, the *ortho*-phenyl decorated ligand **G-TQPy-3** showed a slight enhancement over ligand **G-TQPy-1**. This enhancement is characterized by a less intense metal-to-ligand charge-transfer (MLCT) band, implying a charge transfer in the coordination structure where Cu(I) is oxidized to a relatively high valence state. The phosphorescence emission spectra of the chiral copper complexes in solution (Scheme 4f) revealed a small blue-shift for the complex of **G-TQPy-3** in comparison with **G-TQPy-1** (508 nm *vs.* 513 nm), but the corresponding chiral copper acetylide complexes exhibited a more intense signal, showing that the anionic alkyne is a strong ligand for forming the photocatalytic species. In addition, the ligated guanidine reduces the lifetime of excited copper(I) acetylide (from $\tau = 15.95$ μs to 5.25 μs),[26] but it remains longer than that of species in the singlet excited state to support the redox process (see ESI for details†). It is rationalized that the excited chiral copper complexes undergo intersystem crossing to become triplet excited-state metal complexes, acting as a photo-reductant to undergo single-electron transfer with the oxime.

Cyclic voltammetry was performed on an MeCN solution of each complex in order to probe their electronic properties in the ground state. The voltammograms are given in the ESI† and the relevant potentials are listed in Scheme 4g. The measurements

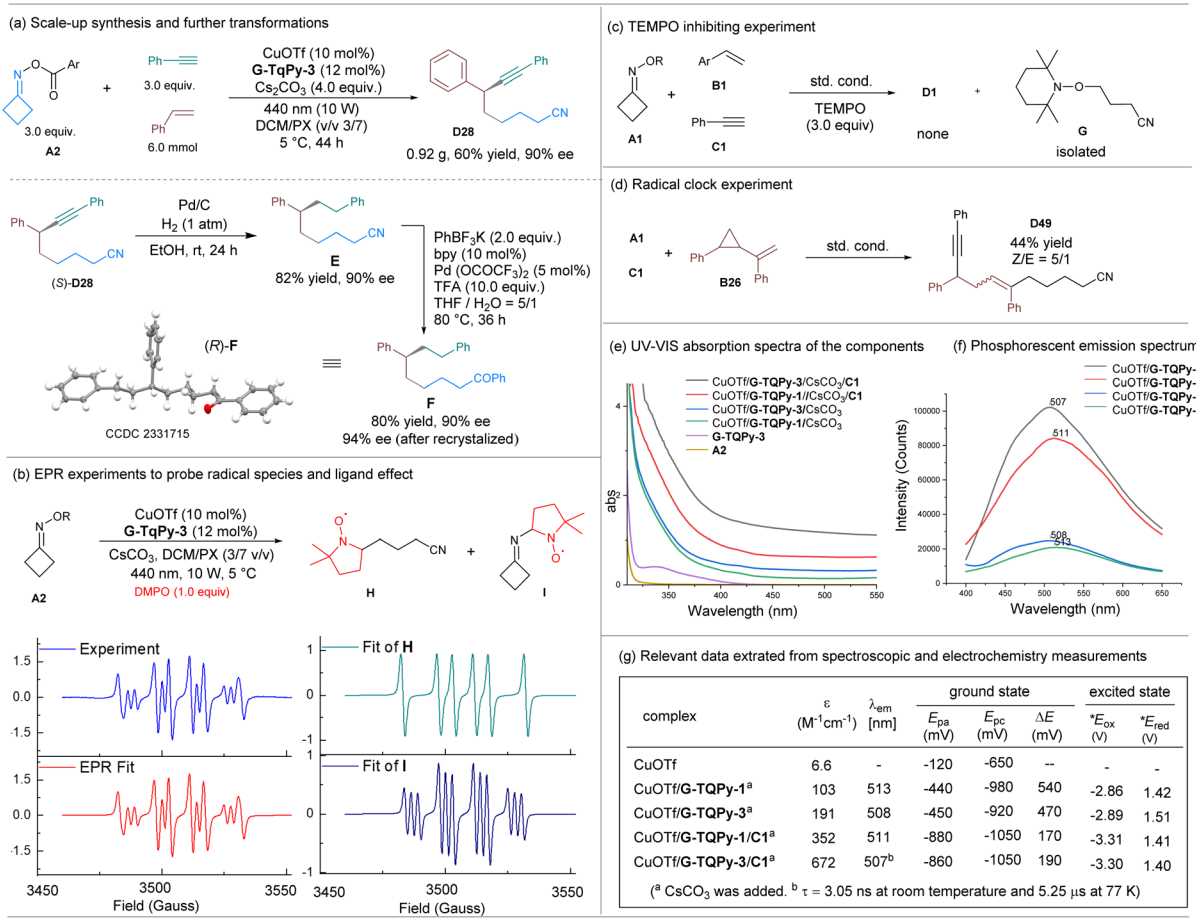

(g) Relevant data extrated from spectroscopic and electrochemistry measurements

complex	ε ($M^{-1}cm^{-1}$)	λ_{em} [nm]	ground state E_{pa} (mV)	ground state E_{pc} (mV)	ground state ΔE (mV)	excited state $^*E_{ox}$ (V)	excited state $^*E_{red}$ (V)
CuOTf	6.6	-	-120	-650	--	-	-
CuOTf/**G-TQPy-1**[a]	103	513	-440	-980	540	-2.86	1.42
CuOTf/**G-TQPy-3**[a]	191	508	-450	-920	470	-2.89	1.51
CuOTf/**G-TQPy-1**/C1[a]	352	511	-880	-1050	170	-3.31	1.41
CuOTf/**G-TQPy-3**/C1[a]	672	507[b]	-860	-1050	190	-3.30	1.40

([a] $CsCO_3$ was added. [b] τ = 3.05 ns at room temperature and 5.25 μs at 77 K)

Scheme 4 Synthetic application and mechanistic investigation.

showed that oxime **A2** has a low E_{red} (−2.44 V_{SCE}), implying that a strongly reductive catalyst is required to initiate iminyl radical generation. Hwang and coworkers have evaluated the redox potential of excited copper(I) acetylide to be −2.048 V_{SCE} in CH_3CN, with a long lifetime.[26] A pseudo-reversible oxidation wave of CuOTf was observed above −1.0 V *versus* SCE, which can be assigned to the Cu(II)/Cu(I) redox couple.

The guanidine-ligated copper complexes (**G-TQPy-1** and **G-TQPy-3**) showed similar E_{ap}/E_{cp}, as did the related chiral copper acetylide complexes. The chiral copper acetylide species have lower oxidation potential than the corresponding chiral precursors. The difference between the redox waves (ΔE) is much smaller for the chiral copper acetylide species than for the precursors. This implies that a flattening of the coordination sphere in the guanidine–ligand–copper catalysts occurs slightly when the distorted Cu(I) acetylide is oxidized to square planar Cu(II), owing to the similar coordination cage. In addition, a rather prominent reduction wave (below −2.1 V_{SCE}) is displayed for the guanidine–copper complexes, corresponding to one-electron ligand-centred reduction, where ligand **G-TQPy-3** itself exhibits multiple reduction waves (see the ESI for details†). The oxidative potential of the excited copper complexes was calculated (Scheme 4g) based on their excitation and emission profiles. This redox potential is sufficiently higher than that of oxime **A2** (−2.44 V_{SCE}). Therefore, in connection with the photophysical properties, SET from a photoexcited triplet chiral copper(I) phenylacetylide to the oxime is exothermic and can occur smoothly.

Based on the above mechanistic data, a plausible mechanism is proposed in Scheme 5. In the presence of a base and the basic tridentate ligand **G-TQPy-3**, a chiral anionic guanidine–

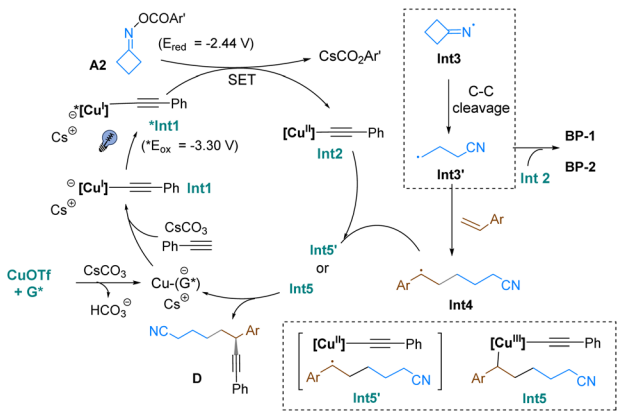

Scheme 5 Proposed catalytic cycle.

amide copper(I) acetylide complex forms. Upon light irradiation, it reaches the triplet state ***Int1**, acting as a strong reductant to perform a SET process with oxime ester **A2**. Thus, square planar copper(II) acetylide **Int2** and an iminyl radical *via* fragmentation are generated, releasing the cesium carboxylate. The iminyl radical **Int3** transforms into cyanoalkyl radical **Int3′** *via* carbon–carbon cleavage, then is trapped by the alkene to give rise to **Int4**. Otherwise, the cross coupling with copper species **Int2** will generate two-component byproducts. The enantioselective coupling between **Int4** and **Int2** may proceed *via* elimination of copper(III) species **Int5** or *via* radical substitution pathways, which is hard to clarify at present. This affords the cyanoalkylalkynylation product with release of the copper(I) species.

Conclusions

In summary, we disclose that a properly designed chiral copper complex with a hybrid tridentate ligand enables photocatalytic asymmetric cyanoalkylalkynylation of olefins using cycloketone oxime esters as the precursors. The ligand, based on a guanidine–amide embellished with a (6-phenylpyridin-2-yl)methanyl group, allows ready electron transfer with lower reorganization energy during the redox processes of the copper acetylide in the excited state. The stereoinduction in the $C(sp^3)$–C(sp) bond formation is also well-controlled with the readily accessible new ligand. The system permits a broad substrate scope with good functional group tolerance, allowing construction of a series of enantiomerically enriched alkyne–nitrile derivatives. We believe that this ligand will bring more opportunities to the development of asymmetric cross-coupling chemistry with detailed studies to understand the spectroscopic origins and the structure–property relationships.

Data availability

Further details of experimental procedure, ^{1}H, $^{13}C\{^{1}H\}$ and $^{19}F\{^{1}H\}$ NMR, HPLC and UPC^2 spectra, and X-ray crystallographic data for **F**, are available in the ESI.†

Author contributions

S. X. performed the experiments. J. B. L. repeated some experiments. Q. T. participated in the article discussions. X. M. F. and X. H. L. supervised the project.

Conflicts of interest

There are no conflicts to declare.

Acknowledgements

We thank the National Natural Science Foundation of China (22188101), and Sichuan University (2020SCUNL204) for financial support. We are grateful to Dr Yuqiao Zhou (Sichuan University) for the X-ray single-crystal diffraction analysis and Dr Hanjiao Chen (Sichuan University) for the EPR measurement and simulation.

Notes and references

1 For selected reviews of alkene difunctionalization:(*a*) L. M. Wickham and R. Giri, *Acc. Chem. Res.*, 2021, **54**, 3415–3437; (*b*) M. Patel, B. Desai, A. Sheth, B. Z. Dholakiya and T. Naveen, *Asian J. Org. Chem.*, 2021, **10**, 3201–3232; (*c*) Z. L. Li, G. C. Fang, Q. S. Gu and X. Y. Liu, *Chem. Soc. Rev.*, 2020, **49**, 32–48; (*d*) J. Huang and Z. M. Chen, *Chem.–Eur. J.*, 2022, **28**, e202201519.

2 (*a*) L. Song, L. Cai, L. Gong and E. V. Van der Eycken, *Chem. Soc. Rev.*, 2023, **52**, 2358–2376; (*b*) M. Mohar, S. Ghosh and A. Hajra, *Chem. Rec.*, 2023, **23**, e202300121; (*c*) P. Gao, Y. J. Niu, F. Yang, L. N. Guo and X. H. Duan, *Chem. Commun.*, 2022, **58**, 730–746.

3 (*a*) X. Y. Dong, J. T. Cheng, Y. F. Zhang, Z. L. Li, T. Y. Zhan, J. J. Chen, F. L. Wang, N. Y. Yang, L. Ye, Q. S. Gu and X. Y. Liu, *J. Am. Chem. Soc.*, 2020, **142**, 9501–9509; (*b*) Y. Zhang, Y. Sun, B. Chen, M. Xu, C. Li, D. Zhang and G. Zhang, *Org. Lett.*, 2020, **22**, 1490–1494.

4 For selected examples of Togni reagents: (*a*) F. Wang, D. Wang, X. Wan, L. Wu, P. Chen and G. Liu, *J. Am. Chem. Soc.*, 2016, **138**, 15547–15550; (*b*) L. Fu, S. Zhou, X. Wan, P. Chen and G. Liu, *J. Am. Chem. Soc.*, 2018, **140**, 10965–10969; (*c*) L. Wu, F. Wang, X. Wan, D. Wang, P. Chen and G. Liu, *J. Am. Chem. Soc.*, 2017, **139**, 2904–2907.

5 S. Sakurai, A. Matsumoto, T. Kano and K. Maruoka, *J. Am. Chem. Soc.*, 2020, **142**, 19017–19022.

6 W. Sha, L. Deng, S. Ni, H. Mei, J. Han and Y. Pan, *ACS Catal.*, 2018, **8**, 7489–7494.

7 Z. H. Zhang, H. Wei, Z. L. Li and X. Y. Liu, *Synlett*, 2021, **32**, 362–369.

8 M. Eckhardt and G. C. Fu, *J. Am. Chem. Soc.*, 2003, **125**, 13642–13643.

9 A. Sagadevan and K. C. Hwang, *Adv. Synth. Catal.*, 2012, **354**, 3421–3427.

10 (*a*) X. Y. Dong, Z. L. Li, Q. S. Gu and X. Y. Liu, *J. Am. Chem. Soc.*, 2022, **144**, 17319–17329; (*b*) C. Gui, T. Zhou, H. Wang, Q. Yan, W. Wang, J. Huang and F. Chen, *Chin. J. Org. Chem.*, 2023, **43**, 2647–2663; (*c*) X. Mo, R. Guo and G. Zhang, *Chin. J. Chem.*, 2023, **41**, 481–489; (*d*) C. Huang, Z. Wan, A. Zhu and C. Chen, *Chin. J. Chem.*, 2024, **42**, 1161–1174.

11 X. Y. Dong, Y. F. Zhang, C. L. Ma, Q. S. Gu, F. L. Wang, Z. L. Li, S. P. Jiang and X. Y. Liu, *Nat. Chem.*, 2019, **11**, 1158–1166.

12 (*a*) W. Yin and X. Wang, *New J. Chem.*, 2019, **43**, 3254–3264; (*b*) D. S. Lee, V. K. Soni and E. J. Cho, *Acc. Chem. Res.*, 2022, **55**, 2526–2541; (*c*) X. Y. Yu, J. R. Chen and W. J. Xiao, *Chem. Rev.*, 2021, **121**, 506–561.

13 J. Boivin, E. Fouquet and S. Z. Zard, *J. Am. Chem. Soc.*, 1991, **113**, 1055–1057.

14 For selected examples of cycloketone oxime esters:(*a*) X. Y. Yu, Q. Q. Zhao, J. Chen, J. R. Chen and W. J. Xiao, *Angew. Chem., Int. Ed.*, 2018, **57**, 15505–15509; (*b*) H. Qian,

J. Chen, B. Zhang, Y. Cheng, W. J. Xiao and J. R. Chen, *Org. Lett.*, 2021, **23**, 6987–6992; (*c*) P. Z. Wang, Y. J. Liang, X. Wu, W. Guan, W. J. Xiao and J. R. Chen, *ACS Catal.*, 2022, **12**, 10925–10937; (*d*) X. J. Xu, Z. M. Chi, R. Rui, Z. Zhang, H. Z. Li and X. Y. Liu, *Adv. Synth. Catal.*, 2024, **366**, 2607–2612; (*e*) J. Chen, B. Q. He, P. Z. Wang, X. Y. Yu, Q. Q. Zhao, J. R. Chen and W. J. Xiao, *Org. Lett.*, 2019, **21**, 4359–4364; (*f*) J. Chen, P. Z. Wang, B. Lu, D. Liang, X. Y. Yu, W. J. Xiao and J. R. Chen, *Org. Lett.*, 2019, **21**, 9763–9768; (*g*) D. Golagani, S. Ajmeera, W. Erb, F. Mongin and S. M. Akondi, *Chem. Commun.*, 2023, **59**, 9259–9262.

15 (*a*) C. Sandoval-Pauker, G. Molina-Aguirre and B. Pinter, *Polyhedron*, 2021, **199**, 115105; (*b*) J. Beaudelot, S. Oger, S. Peruško, T. A. Phan, T. Teunens, C. Moucheron and G. Evano, *Chem. Rev.*, 2022, **122**, 16365–16609.

16 P. Z. Wang, Z. Zhang, M. Jiang, J. R. Chen and W. J. Xiao, *Angew. Chem., Int. Ed.*, 2024, **63**, e202411469.

17 J. K. McCusker, *Science*, 2019, **363**, 484–488.

18 G. Zhang, H. Yi, G. Zhang, Y. Deng, R. Bai, H. Zhang, J. T. Miller, A. J. Kropf, E. E. Bunel and A. Lei, *J. Am. Chem. Soc.*, 2014, **136**, 924–926.

19 H. D. Zuo, S. S. Zhu, W. J. Hao, S. C. Wang, S. J. Tu and B. Jiang, *ACS Catal.*, 2021, **11**, 6010–6019.

20 (*a*) A. Hossain, A. Bhattacharyya and O. Reiser, *Science*, 2019, **364**, eaav9713; (*b*) M. J. Genzink, J. B. Kidd, W. B. Swords and T. P. Yoon, *Chem. Rev.*, 2022, **122**, 1654–1716.

21 B. Dicke, A. Hoffmann, J. Stanek, M. S. Rampp, B. Grimm-Lebsanft, F. Biebl, D. Rukser, B. Maerz, D. Göries, M. Naumova, M. Biednov, G. Neuber, A. Wetzel, S. M. Hofmann, P. Roedig, A. Meents, J. Bielecki, J. Andreasson, K. R. Beyerlein, H. N. Chapman, C. Bressler, W. Zinth, M. Rübhausen and S. Herres-Pawlis, *Nat. Chem.*, 2018, **10**, 355–362.

22 For reviews on guanidine catalysts:(*a*) W. D. Cao, X. H. Liu and X. M. Feng, *Chin. Chem. Lett.*, 2018, **29**, 1201–1208; (*b*) S. X. Dong, X. M. Feng and X. H. Liu, *Chem. Soc. Rev.*, 2018, **47**, 8525–8540; (*c*) X. H. Liu, S. X. Dong, L. L. Lin and X. M. Feng, *Chin. J. Chem.*, 2018, **36**, 791–797.

23 For selected examples of chiral guanidine–metal complex catalysis: (*a*) Y. Tang, Q. G. Chen, X. H. Liu, G. Wang, L. L. Lin and X. M. Feng, *Angew. Chem., Int. Ed.*, 2015, **54**, 9512–9516; (*b*) S. Ruan, X. Zhong, Q. G. Chen, X. M. Feng and X. H. Liu, *Chem. Commun.*, 2020, **56**, 2155–2158; (*c*) Q. G. Chen, Y. Tang, T. Y. Huang, X. H. Liu, L. L. Lin and X. M. Feng, *Angew. Chem., Int. Ed.*, 2016, **55**, 5286–5289; (*d*) Q. G. Chen, L. H. Xie, Z. J. Li, Y. Tang, P. Zhao, L. L. Lin, X. M. Feng and X. H. Liu, *Chem. Commun.*, 2018, **54**, 678–681; (*e*) S. S. Guo, P. Dong, Y. S. Chen, X. M. Feng and X. H. Liu, *Angew. Chem.*, 2018, **130**, 17094–17098; (*f*) Y. Tang, J. Xu, J. Yang, L. L. Lin, X. M. Feng and X. H. Liu, *Chem*, 2018, **4**, 1658–1672; (*g*) L. F. Hu, J. Z. Li, Y. Y. Zhang, X. M. Feng and X. H. Liu, *Chem. Sci.*, 2022, **13**, 4103.

24 J. Z. Li, L. C. Ning, Q. F. Tan, X. M. Feng and X. H. Liu, *Org. Chem. Front.*, 2022, **9**, 6312–6318.

25 CCDC 2331715 for **F** contains the supplementary crystallographic data for this paper. These data are provided free of charge by the joint Cambridge Crystallographic Data Centre and Fachinformationszentrum Karlsruhe Access Structures service.

26 A. Sagadevan, A. Ragupathi and K. C. Hwang, *Angew. Chem., Int. Ed.*, 2015, **54**, 13896–13901.